Analytica Chimica Acta 933 (2016) 43–49

Contents lists available at ScienceDirect

Analytica Chimica Acta

journal homepage: www.elsevier.com/locate/aca

A new and consistent parameter for measuring the quality of multivariate analytical methods: Generalized analytical sensitivity

Wallace Fragoso [a, b], Franco Allegrini [b], Alejandro C. Olivieri [b, *]

[a] Departamento de Química Analítica, Facultad de Ciencias Bioquímicas y Farmacéuticas, Universidad Nacional de Rosario, Instituto de Química de Rosario (IQUIR-CONICET), Suipacha 531, Rosario S2002LRK, Argentina
[b] Universidade Federal da Paraíba (UFPB), Centro de Ciências Exatas e da Natureza, Departamento de Química, Castelo Branco, João Pessoa, PB, Brazil

HIGHLIGHTS

- Sensitivity for various multivariate calibration methods is studied.
- Different error structures are considered.
- Generalized analytical sensitivity is proposed as a new figure of merit.
- The new parameter allows better comparison among calibration methods.

GRAPHICAL ABSTRACT

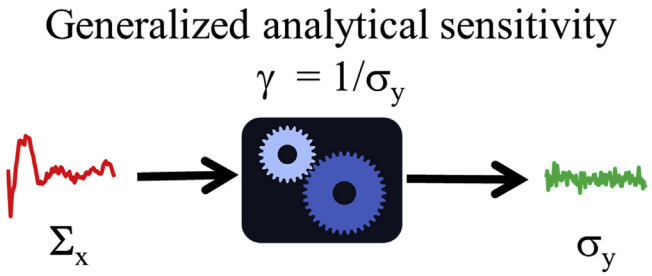

ARTICLE INFO

Article history:
Received 24 March 2016
Received in revised form
17 June 2016
Accepted 19 June 2016
Available online 21 June 2016

Keywords:
Multivariate calibration
Analytical figures of merit
Sensitivity
Analytical sensitivity
Method comparison

ABSTRACT

Generalized analytical sensitivity (γ) is proposed as a new figure of merit, which can be estimated from a multivariate calibration data set. It can be confidently applied to compare different calibration methodologies, and helps to solve literature inconsistencies on the relationship between classical sensitivity and prediction error. In contrast to the classical plain sensitivity, γ incorporates the noise properties in its definition, and its inverse is well correlated with root mean square errors of prediction in the presence of general noise structures. The proposal is supported by studying simulated and experimental first-order multivariate calibration systems with various models, namely multiple linear regression, principal component regression (PCR) and maximum likelihood PCR (MLPCR). The simulations included instrumental noise of different types: independently and identically distributed (*iid*), correlated (pink) and proportional noise, while the experimental data carried noise which is clearly non-*iid*.

1. Introduction

Starting from the seminal work of Lorber [1], the estimation of analytical figures of merit in multivariate calibration has become an active research field in analytical chemistry. Some recent developments show the continuous interest in this area by the analytical community [2–7]. In particular, the derivation of a generalized expression for estimating the important sensitivity parameter in a general calibration scenario has been possible [3], with a twofold consequence. On one hand, the sensitivity has traditionally been considered as a good indicator for comparing methodologies in terms of analytical performance, thus any advance in the estimation of multivariate and multiway sensitivity is welcome [3]. On the other, knowledge of the sensitivity provides access to additional figures which depend on the latter, such as prediction uncertainty and detection capabilities [3,5].

* Corresponding author.
E-mail address: olivieri@iquir-conicet.gov.ar (A.C. Olivieri).

http://dx.doi.org/10.1016/j.aca.2016.06.022
0003-2670/

The classical definition of sensitivity is based on the idea of a signal change for a given change in analyte concentration [8]. This concept is valid in univariate calibration, where the sensitivity is numerically equal to the slope of the calibration graph [8]. It is also suitable in first-order multivariate calibration, provided 'signal' is replaced by 'net analyte signal' [1]. However, the analogous concept of net signal cannot be successfully extended to multiway calibration, for reasons already discussed [3].

It has been increasingly clear that a new definition of sensitivity was required, and this was possible in the framework of uncertainty propagation [3]. When the sensitivity is numerically defined as the ratio of signal to concentration uncertainties, a completely general expression can be derived, valid for univariate, first-order multivariate and higher-order multiway calibrations, including cases where the second-order advantage is achieved. This new definition is completely consistent with the classical univariate and first-order expressions, and is also in agreement with extensive noise addition simulations [3].

However, at the heart of the general sensitivity expression, derived from uncertainty propagation arguments, rests the assumption of a particular structure for the signal noise: it should be identically and independently distributed (*iid*). Operationally, a small amount of *iid* noise is numerically added to the test sample signal, and analyte concentration is predicted with its corresponding uncertainty (Fig. 1A). It is postulated that the small noise added to the signal is simply a probe to monitor the uncertainty propagation behavior, and should not necessarily reflect the real noise structure of the instrumental signals [3]. It should be noted that the small *iid* noise is only added to the test sample signal, keeping the calibration model precise. In this way, uncertainty only propagates from the instrumental signal for the test sample and not from the calibration signals or concentrations.

The question remains whether the sensitivity parameter is useful for one of its intended purposes, i.e., method performance comparison, in the case of real systems showing signal noise structures different than the ideal *iid*. In light of the presently discussed results, the answer is negative. In this report, an alternative figure of merit is proposed, which is better correlated with analytical performance and can be estimated only from the calibration data set. It is a generalization of the already known analytical sensitivity (γ) [9,10], here extended to any noise structure and calibration methodology [11]. The classical parameter γ, defined as the ratio between univariate calibration slope and standard measurement error, has been proposed for method comparison instead of the slope, because the former is independent

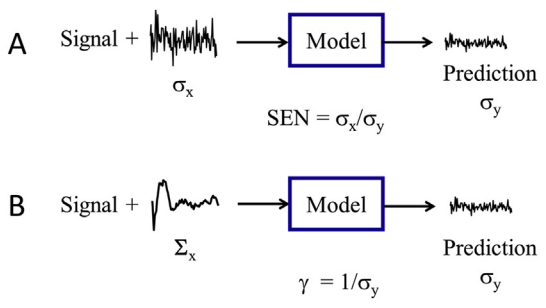

Fig. 1. Schematic representation of the uncertainty propagation approach to sensitivity analysis. A) *iid* noise (represented by its standard deviation σ_x) is introduced only in the test sample signal, keeping the model precise, and the sensitivity (SEN) is computed as the ratio of input signal noise to output concentration noise (σ_y). B) Real non-*iid* noise (represented by its error variance-covariance matrix Σ_x) is added only to the test signal, keeping the model precise, and the generalized analytical sensitivity (γ) is estimated as the inverse of the output concentration noise. See text for the meanings of σ_x, σ_y and Σ_x.

on the type of instrumental signal [9]. We generalize the definition of γ for multivariate methods, as the inverse of the concentration uncertainty generated by real noise propagation, and show it to be an excellent parameter for method comparison in the case of general noise structures. Fig. 1B adequately illustrates the presently proposed definition, noting that, as in Fig. 1A, the noise is only added to the instrumental signal for the test sample, keeping the calibration model precise, i.e., avoiding propagation from errors in calibration signals or concentrations.

To support our proposal, we use a set of simulated first-order data carrying *iid*, correlated and proportional noise, and also experimental data including non-*iid* noise. They were processed using the following multivariate tools: (1) multiple linear regression (MLR) [12] of signals for a few wavelengths, which were carefully selected with the aid of the successive projection algorithm (SPA) [13], (2) principal component regression (PCR) [14] and (3) maximum likelihood PCR (MLPCR) [15,16]. The purpose of using MLR was to assess the performance when calibration is built using a few wavelengths, which in principle presents significantly smaller sensitivity in comparison with full spectral latent methods such as PCR and MLPCR, yet sometimes producing comparable or even better analytical results [17,18]. On the other hand, MLPCR was applied because of its known ability to cope with noise structures other than the *iid* one [15,16], and to check whether this improved analytical ability is correlated with the corresponding numerical sensitivity value.

In sum, the present proposal has the following purposes: (1) providing a figure of merit which could be used to compare different calibration models with confidence, and derived only from the calibration data set, i.e., not requiring an independent set of samples for its estimation, and (2) solving inconsistencies in literature reports where calibration with a few sensors provided better analytical results but lower classical sensitivity.

2. Theory

2.1. Calibration methodologies

The theory behind MLR and PCR calibration is well known [12,14]. SPA and MLPCR are briefly described in the Supplementary Material. Partial least-squares (PLS) results are not shown, as they were almost identical to those furnished by PCR, but are included in the Supplementary Material.

In all cases, a calibration data matrix $\mathbf{X}$ (size $I \times J$, I = number of calibration samples, J = number of sensors or wavelengths) and a calibration concentration vector for the analyte of interest $\mathbf{y}_{cal}$ (size $I \times 1$) were submitted to the calibration phase with a given multivariate model. This yields the regression vector $\mathbf{b}$ (size $J \times 1$), which permits analyte quantitation through the usual predictive expression $\hat{y} = \mathbf{x}^T\mathbf{b}$ ($\mathbf{x}$ is the test sample spectrum, size $J \times 1$, the hat '^' implying predicted value).

2.2. Uncertainty propagation

In a recent work, Allegrini et al. presented a general scheme to estimate sample dependent prediction uncertainties in first-order multivariate calibration [19]. Because the *iid* hypothesis for measurement errors is not always valid for real data sets, new expressions were developed to take into account the specific noise structure. The overall prediction variance (σ_y^2) in multivariate models can be estimated by a sum of three contributing terms: (1) the variance from instrumental signals measured for the test sample, (2) the variance from instrumental signals measured for the calibration set of samples and (3) the variance in nominal concentrations of the analyte or property of interest [2,19]. The

following general equation adequately covers these contributions to σ_y^2 [19]:

$$\sigma_y^2 = \mathbf{b}^T\boldsymbol{\Sigma}_x\mathbf{b} + h\mathbf{b}^T\boldsymbol{\Sigma}_{Xeff}\mathbf{b} + h\sigma_{ycal}^2 \quad (1)$$

where h is the test sample leverage, σ_{ycal}^2 is the variance in calibration concentrations, $\mathbf{b}$ is the vector of regression coefficients, $\boldsymbol{\Sigma}_x$ is the error covariance matrix for the test sample signals and $\boldsymbol{\Sigma}_{Xeff}$ is an effective error covariance matrix for the calibration signals. The latter is a weighted average of the error covariance matrices for all calibration samples, the weight being a specific element of the sample leverage vector $\mathbf{h}$. For details see Ref. [19].

When all error covariance matrices are equal, $\boldsymbol{\Sigma}_{Xeff} = \boldsymbol{\Sigma}_x$ in Equation (1), as for correlated homoscedastic noise such as the so-called pink noise [19]. Finally, when the noise is *iid*, both $\boldsymbol{\Sigma}_x$ and $\boldsymbol{\Sigma}_{Xeff}$ become diagonal and equal to $\sigma_x^2\mathbf{I}$, where σ_x^2 is the (constant) variance of all instrumental signals and $\mathbf{I}$ is a $J \times J$ identity matrix. In such a case, Equation (1) collapses to:

$$\sigma_y^2 = \sigma_x^2\mathbf{b}^T\mathbf{b} + h\sigma_x^2\mathbf{b}^T\mathbf{b} + h\sigma_{ycal}^2 \quad (2)$$

Since the product ($\mathbf{b}^T\mathbf{b}$) is numerically equal to the inverse squared sensitivity [2]:

$$SEN = \frac{1}{(\mathbf{b}^T\mathbf{b})^{1/2}} \quad (3)$$

and replacing the latter result in Equation (2) leads to:

$$\sigma_y^2 = \sigma_x^2/SEN^2 + h\sigma_x^2/SEN^2 + h\sigma_{ycal}^2 \quad (4)$$

The relative effect of the three terms in Equation (4) have been previously studied, finding that the first term usually dominates the prediction uncertainty (see Fig. 3 of Ref. [19], where the position of the points corresponding to the second and third terms are always at lower values with respect to the points corresponding to the first term). Thus, according to Equation (4), one would expect a correlation between predictive ability, measured by the average prediction error, and the inverse of the plain sensitivity (SEN^{-1}). However, this would be true provided the error structure is *iid*, as clearly shown in the above expressions. What actually occurs when the real noise structure deviates from the *iid* situation, and what is the relationship between average prediction error and SEN^{-1} is obviously less clear. The remaining of this report is devoted to explore the connection.

It should be noticed that a procedure for estimating prediction error has been formulated by Andersen and Bro [20], proposing an equation similar to (4), but incorporating the so-called model errors. The latter include model deviations such as lack of linearity, and require the estimation of concentration prediction errors for a set of samples. This issue is certainly important, and deserves future detailed analysis, but is beyond the present purpose, where we apply error propagation to the model predictive expression, assuming only that random errors are present.

2.3. Software

All calculations were made using MATLAB [21]. Variable selection was performed using the graphical interface SPA_GUI.p, available in the authors' homepage http://www.ele.ita.br/~kawakami/spa/(accessed February 2016). MLPCR was performed using the algorithm developed by Wentzell and Lohnes [22]. Pink noise and the associated error covariance matrix were calculated by a MATLAB routine provided by Wentzell [19]. PCR was implemented with an in-house MATLAB routine.

3. Data sets

3.1. Simulated data

For the simulated study, 15 independent calibration data sets, named S1 to S15 were built, with 200 sensors and 100 samples each. Fig. 2A shows the spectra of the four pure components and one representative mixture. The concentrations were chosen randomly between 0 and 1. The noise in concentrations was included adding a random value between 0 and 1 times a noise level factor (10^{-3} units). For each calibration system, two new sets were built by addition of either *iid* or pink noise. The error covariance matrix of the *iid* noise was calculated by:

$$\boldsymbol{\Sigma}_x = 1 \times 10^{-4} NL_x \max(\mathbf{X}_0)\mathbf{I} \quad (5)$$

where NL_x is the spectral noise level, equal to 1 for S1 to S10 (these systems differ in the specific component concentrations), and to 1.2, 1.4, 1.6, 1.8 and 2.0 units for S11, S12, S13, S14 and S15, respectively, $\max(\mathbf{X}_0)$ is the maximum intensity value in the noiseless spectral matrix $\mathbf{X}_0$, and $\mathbf{I}$ is a 200 × 200 identity matrix.

The pink noise and the associated error covariance matrix were computed using the same NL_x values defined for the *iid* noise. Validation data sets were built in the same way. Fig. 2B shows a representative sample without noise, with *iid* noise and with pink noise. Short range correlations in the pink noise spectrum are clearly seen in comparison with *iid* noise.

3.2. Experimental data

In this work we use the data set generated by Shreyer et al. [16] to test the application of MLPCR to fluorescence emission spectra. It consists of 5 replicates of 27 mixtures of three polycyclic aromatic hydrocarbons: acenaphthylene (ACE), naphthalene (NAP) and phenanthrene (PHE). A three level, three-factor factorial design was used to build the data set and the samples were scanned in a randomized order of five blocks. The final concentration ranges were 0.10–0.34 mg g^{-1} (ACE), 0.018–0.063 mg g^{-1} (NAP), and 0.0072–0.027 mg g^{-1} (PHE). The emission spectra were obtained through a 1 cm quartz cuvette on a Shimadzu RF-5301PC spectrofluorometer with a xenon lamp excitation source. The excitation wavelength was 278 nm. The emission spectra were measured between 310 and 460 nm with an interval of 0.2 nm. The excitation and emission slit widths were both set to 3.0 nm. For further details see ref. [16].

4. Results and discussion

4.1. Simulations

For all studied systems, we computed the root mean square error of prediction (RMSEP) for the test sets, which is normally used to evaluate the quality of a multivariate model, comparing the predicted and nominal concentrations of a reference set of samples. Lower values of RMSEP are associated with models with a better prediction power. On the other hand, higher sensitivity is intuitively expected for good models. Thus, analysis of the mutual relationship of RMSEP and SEN should allow, in theory, for a comparison among different models.

Fig. 3 shows the RMSEP for analyte 1 in the 15 simulated data sets which involve different noise types (*iid* and pink noise), noise levels and models (SPA-MLR, PCR and MLPCR; the latter is not shown for *iid* noise because in this case it is equivalent to classical PCR). Complementary results for the calibration of the remaining sample components are shown in the Supplementary Material

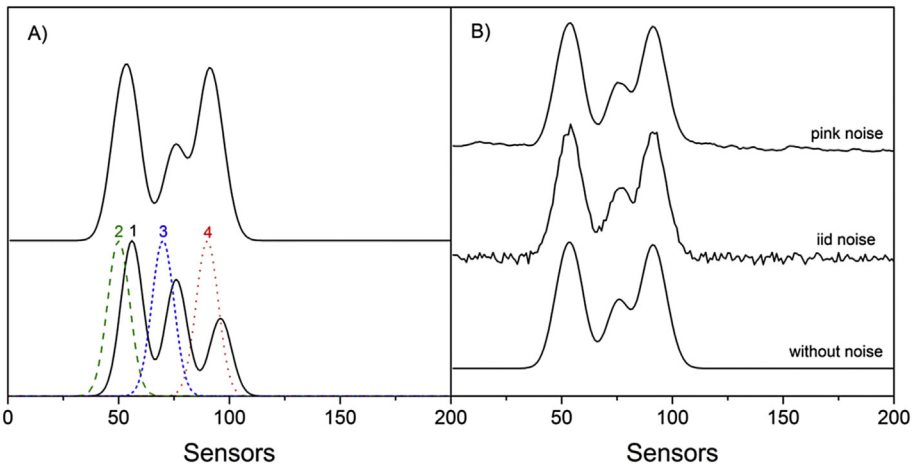

Fig. 2. A) Bottom: simulated spectra of the four pure components. Top: a representative sample spectrum. B) A typical simulated sample without noise and with *iid* and pink noise (as indicated). (For interpretation of the references to colour in this figure legend, the reader is referred to the web version of this article.)

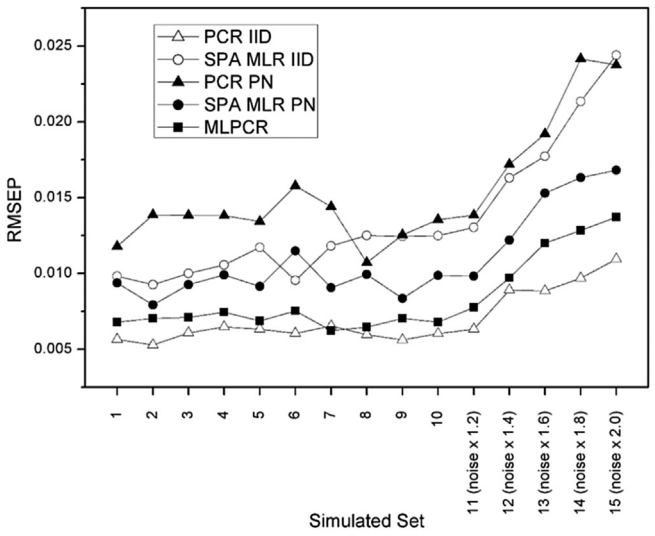

Fig. 3. Root mean square error of prediction (RMSEP) in the simulated data sets. The different methods were applied to systems having *iid* or pink noise, as indicated. MLPCR was only applied to data carrying pink noise, since for *iid* noise it becomes identical to PCR. The level of noise is also indicated (see text).

(Figs. S1–S3). PCR shows better analytical performance in comparison with SPA-MLR for *iid* noise (compare open triangles with open circles in Fig. 3). These are the classically expected results from the known properties of full-wavelength methods (PCR) and those based on a few selected sensors (SPA-MLR).

On the other hand, when pink noise is added, MLPCR leads to the best results (filled squares in Fig. 3), significantly outperforming PCR and SPA-MLR (filled triangles and filled circles respectively in Fig. 3). Since MLPCR was specifically developed to take into account the noise structure, it is not surprising that this model shows better predictive ability when the data set includes correlated noise. Although the literature alerts on the importance of considering the noise structure in the multivariate models [23,24], the current paradigm in analytical chemistry is still to consider the noise as *iid*. It is likely that experimental difficulties in preparing replicate samples, which are needed to estimate the error covariance matrix, may be the most important factor in preserving this paradigm.

Somewhat surprisingly, however, SPA-MLR closely follows MLPCR in analytical performance when pink noise is present (Fig. 3). Therefore, the use of SPA-MLR can be a good option when the noise is known to be correlated, especially since knowledge of the error covariance matrix is not necessary to build an MLR model. Since the latter includes data for a few wavelengths which are not necessarily contiguous, the effect of short-range correlations is minimized, leading to better predictions than PCR, which resorts to full spectral data, where the correlation effect may be significant. These observations may be the key to understand why sometimes SPA-MLR presents better performance than PCR, even when SEN is significantly larger for this latter method [17,18].

Fig. 4A and B shows the relationship between inverse sensitivity and RMSEP. For *iid* noise (Fig. 4A), PCR presents lower RMSEP values and concomitant larger sensitivities than SPA-MLR for comparable noise levels. The sensitivity is virtually constant within specific models, although they show different RMSEP, which are due to different noise levels. SPA-MLR shows a larger dispersion in SEN values, since the selected variables change with the calibration data set and noise level. This is due to the fact that a fair comparison requires SPA selection to be done in the manner that leads to the best set of selected sensors for each system.

On the other hand, in the case of pink noise RMSEP and SEN^{-1} do not follow any logical relationship among different models (Fig. 4B). PCR shows the largest RMSEP values, but also the largest SEN values, which is not consistent. On the other hand, MLPCR presents the best RMSEP values, but intermediate values of SEN. Finally, SPA-MLR, with intermediate RMSEP values, displays the lowest sensitivity.

Analogous results to those shown in Fig. 4 were obtained for the remaining sample components beyond analyte 1 (see Supplementary Material, Figs. S4–S6). Additional systems were studied by adding proportional noise, which is not correlated but heteroscedastic (results not shown) [22]. The trends are similar to those discussed above for *iid* noise, in the sense that the RMSEP is logically correlated with SEN^{-1}, and, as expected, MLPCR provides the best analytical results, because the error structure is incorporated into the calibration model.

In contrast to the inverse sensitivity, the mean standard deviation (MSD), defined as the average of the prediction uncertainties estimated using Equation (1) for the test set, is well correlated with RMSEP. This is shown in Fig. 4C and D as a function of RMSEP across all studied models and noise structures. This confirms the validity of the recently developed expression (2) for prediction uncertainty when the noise structure deviates from the *iid* paradigm [19], and led us to propose a new figure of merit for method comparison (see below).

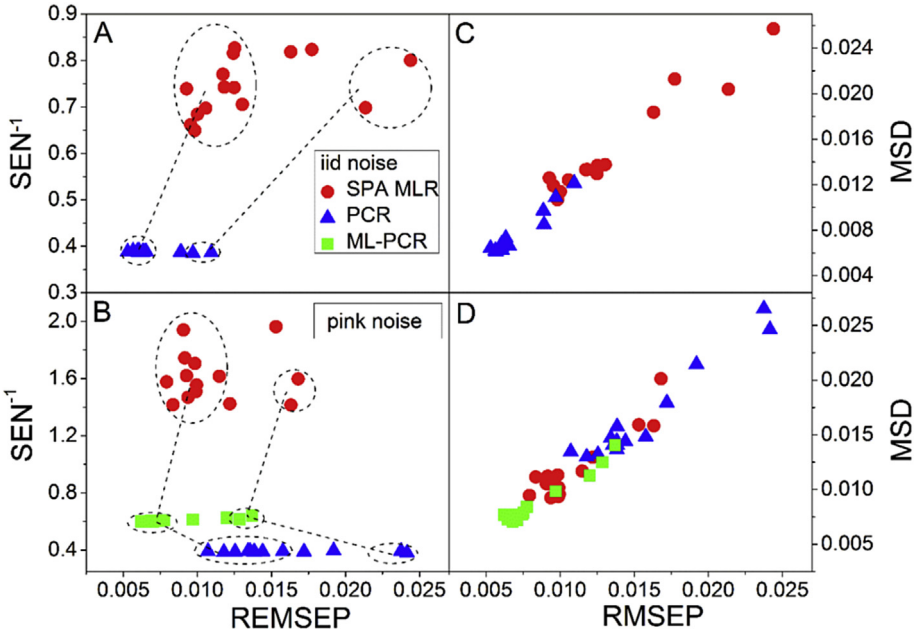

Fig. 4. A) Inverse sensitivity parameter SEN^{-1} estimated with Equation (3) as a function of root mean square error of prediction (RMSEP) in the case of *iid* noise. B) Same as A) for pink noise. C) Mean standard deviation (MSD) calculated with Equation (1) by averaging the σ_y values for the test set as a function of RMSEP in the case of *iid* noise. D) Same as C for pink noise. In plots A) and B) the dotted lines group results for the same noise level (left, minimum, right, maximum).

4.2. Experimental results

Fig. 5 shows a representative experimental spectrum and the selected variables by SPA-MLR for the three analytes. Fourteen variables were selected for ACE, eighteen for NAP and eight for PHE. The selection of significantly more variables than the number of sample components in the case of ACE and NAP (Fig. 5) probably occurs because of the large degree of spectral overlap among sample components.

Table 1 shows RMSEP, SEN and MSD values for SPA-MLR, PCR and MLPCR models of the experimental data set. Included are individual contributions of the first two terms to the prediction variance, derived from uncertainty in instrumental signals, showing that the first term is dominant, as was the case with the simulations (see above). As can be seen, MLPCR provides the best models judging by the RMSEP criterion, followed by PCR and then by SPA-MLR. However, the SEN values do not agree with these observations, since PCR models show larger SEN values. In this specific case, SPA-MLR does not outperform PCR, but the differences in favor of PCR are not significant, and do not justify the difference in the sensitivity. The most significant error sources in these data have been characterized by Wentzell et al. [23]. The main contributions to the noise structure are: (1) proportional shot noise in fluorescence spectroscopy (heteroscedastic noise where the standard deviation is proportional to the square root of the signal, arising from the Poisson distribution associated with photomultipliers) [22], (2) constant offset noise which arises from cell positioning, and (3) offset noise proportional to the square root of the spectrum. Correlated noise does not dominate the error sources in this case, explaining why SPA-MLR is not better than latent

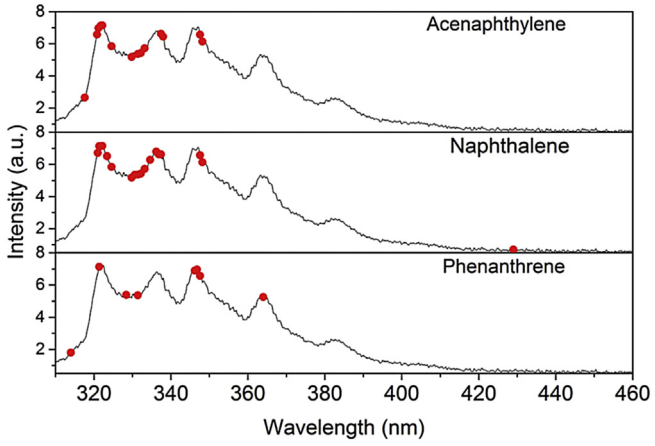

Fig. 5. Variables selected by SPA for MLR calibration of three polycyclic aromatic hydrocarbons (red dots). In the vertical axis, a.u. implies arbitrary units. (For interpretation of the references to colour in this figure legend, the reader is referred to the web version of this article.)

Table 1
Experimental data: figures of merit for three analytes and three different modeling strategies.[a]

	SPA-MLR	PCR	MLPCR
Acenaphthylene			
RMSEP/mg g^{-1}	0.0113	0.0085	0.0079
SEN/FU g mg^{-1}	7.2	21.3	17.0
MSD/mg g^{-1}	0.0111	0.0077	0.0050
MSD^2: ratio of first to second term	8.6	5.0	6.3
Naphthalene			
RMSEP/mg g^{-1}	0.0016	0.0015	0.0012
SEN/FU g mg^{-1}	45.1	206.7	130.4
MSD/mg g^{-1}	0.0016	0.0013	0.0007
MSD^2: ratio of first to second term	5.5	4.7	5.0
Phenanthrene			
RMSEP/mg g^{-1}	4.0×10^{-4}	3.9×10^{-4}	3.1×10^{-4}
SEN/FU g mg^{-1}	200.9	1048.7	541.3
MSD/mg g^{-1}	4.3×10^{-4}	3.9×10^{-4}	2.5×10^{-4}
MSD^2: ratio of first to second term	16	5.1	7.1

[a] RMSEP = root mean square error of prediction, SEN = sensitivity, MSD = mean standard deviation of prediction across the test sample set, FU = fluorescence intensity units. The relative contribution to the value of MSD^2 is given as the ratio of the first to the second term in Equation (2), which represent the uncertainty from the instrumental signals.

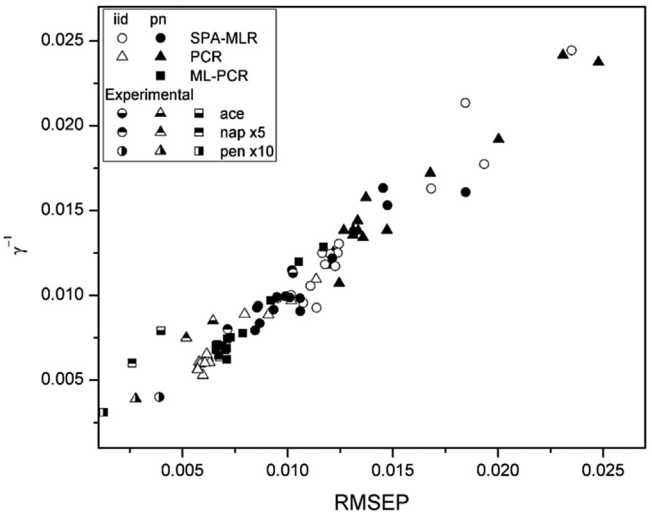

Fig. 6. Inverse generalized analytical sensitivity (γ^{-1}) as a function of root mean square error of prediction (RMSEP), including both simulated (analyte 1) and experimental systems (units are mg g^{-1}), and both *iid* and pink noise structures.

structured methods.

4.3. Generalized analytical sensitivity

The above results appear to indicate that the plain sensitivity parameter is not the best indicator to be used for comparison of the performance of analytical methods. However, the present study suggests that a new figure of merit could replace SEN in this regard, based on the results obtained using the MSD concept. In general, the first term in Equation (1) is sample independent, at least for *iid* and pink noise. According to Fig. 1B, we propose a definition for a generalized analytical sensitivity γ as the inverse of the concentration uncertainty due to the first term of Equation (1):

$$\gamma = \frac{1}{\left(\mathbf{b}^{T}\boldsymbol{\Sigma}_{X}\mathbf{b}\right)^{1/2}} \tag{6}$$

where $\boldsymbol{\Sigma}_X$ is the error covariance matrix for the calibration noise. In this way, γ characterizes the calibration model, since both $\mathbf{b}$ and $\boldsymbol{\Sigma}_X$ correspond to the calibration phase. In the case of proportional noise, which varies with each sample, we suggest to employ the average calibration error covariance matrix in Equation (6), to obtain a sample-independent figure of merit for the calibration model. The use of average error covariance matrices has already been shown to be a good approximation to estimate prediction uncertainties from Equation (1) [19].

Fig. 6 shows the changes in inverse analytical sensitivity (γ^{-1}) as a function of RMSEP for all simulated and experimental models studied in this report (proportional noise results are not shown but follow the same trend observed in this figure). In the case of the simulated systems, Fig. 6 shows the results for analyte 1, while that for the remaining sample components are presented in the Supplementary Material (Figs. S7–S9) for clarity. A nice correlation is clearly appreciated between both statistical indicators in Fig. 6, which leads us to believe that γ is an appropriate parameter for comparing different models in terms of prediction ability in generalized calibration and noise scenarios.

5. Conclusions

Comparison of predictive ability is a necessary activity when developing new analytical methodologies. Although the sensitivity has been traditionally used for this purpose, the present reports shows that this is only valid when the instrumental noise is of a particular type, i.e., independently and identically distributed. In other noise scenarios, however, the sensitivity fails to provide the required answer. A detailed study of the prediction uncertainty under general noise structures shows that it is possible to define a new figure of merit for method comparison. The generalized analytical sensitivity has been proposed for this purpose, and showed to be suitably correlated with analytical performance in a variety of situations.

Acknowledgments

Universidad Nacional de Rosario, CONICET (Consejo Nacional de Investigaciones Científicas y Técnicas, Project No. PIP 0163), ANPCyT (Agencia Nacional de Promoción Científica y Tecnológica, Project No. PICT-2013-0136), and Conselho Nacional de Desenvolvimento Científico e Tecnológico (CNPq) are gratefully acknowledged for financial support. F. A. thanks CONICET and W. F. thanks CNPq for postdoctoral fellowships.

Appendix A. Supplementary data

Supplementary data related to this article can be found at http://dx.doi.org/10.1016/j.aca.2016.06.022.

References

[1] A. Lorber, Error propagation and figures of merit for quantification by solving matrix equations, Anal. Chem. 58 (1986) 1167–1172.
[2] K. Faber, A. Lorber, B.R. Kowalski, Analytical figures of merit for tensorial calibration, J. Chemom. 11 (1997) 419–461.
[3] A.C. Olivieri, N.M. Faber, J. Ferre, R. Boque, J.H. Kalivas, H. Mark, Uncertainty estimation and figures of merit for multivariate calibration, Pure Appl. Chem. 78 (2006) 633–661.
[4] A.C. Olivieri, Analytical figures of merit: from univariate to multiway calibration, Chem. Rev. 114 (2014) 5358–5378.
[5] A.C. Olivieri, G.M. Escandar, Practical Three-way Calibration, Elsevier, Amsterdam, 2014 (Chapter 6).
[6] A.C. Olivieri, S. Bortolato, F. Allegrini, Figures of merit in multiway calibration, in: A. Muñoz de la Peña, H.C. Goicoechea, G.M. Escandar, A.C. Olivieri (Eds.), Data Handling in Science and Technology, Fundamentals and Analytical Applications of Multiway Calibration, Vol. 29, Elsevier, Amsterdam, 2015 (Chapter 13).
[7] Z. Dorkó, T. Verbić, G. Horvai, Selectivity in analytical chemistry, Talanta 139 (2015) 40–49.
[8] K. Danzer, L.A. Currie, Guidelines for calibration in analytical chemistry. Part I. Fundamentals and single component calibration, Pure Appl. Chem. 70 (1998) 993–1014.
[9] R.K. Skogerboe, C.L. Grant, Comments on the definition of the terms sensitivity and detection limit, Spectrosc. Lett. 3 (1970) 215–220.
[10] L. Cuadros Rodríguez, A.M. García Campaña, C. Jiménez Linares, M. Román Ceba, Estimation of performance characteristics of an analytical method using the data set of the calibration experiment, Anal. Lett. 26 (1993) 1243–1258.
[11] Notice that Ref. 10 Defines γ as the ratio of error to slope, i.e., the inverse of ref. 9. We prefer to maintain the latter definition for compatibility with the classical SEN.
[12] D.M. Haaland, E.V. Thomas, Partial least-squares methods for spectral analyses. 1. Relation to other quantitative calibration methods and the extraction of qualitative information, Anal. Chem. 60 (1988) 1193–1202.
[13] M.C.U. Araújo, T.C.B. Saldanha, R.K.H. Galvão, T. Yoneyama, H.C. Chame, V. Visani, The successive projections algorithm for variable selection in spectroscopic multicomponent analysis, Chemom. Intell. Lab. Syst. 57 (2001) 65–73.
[14] S. Wold, K. Esbensen, P. Geladi, Principal component analysis, Chemom. Intell. Lab. Syst. 2 (1987) 37–52.
[15] P.D. Wentzell, D.T. Andrews, D.C. Hamilton, K. Faber, B.R. Kowalski, Maximum likelihood principal component analysis, J. Chemom. 11 (1997) 339–366.
[16] S.K. Schreyer, M. Bidinosti, P.D. Wentzell, Application of maximum likelihood principal components regression to fluorescence emission spectra, Appl. Spectrosc. 56 (2002) 789–796.
[17] M.S. Di Nezio, M.F. Pistonesi, W.D. Fragoso, M.J.C. Pontes, H.C. Goicoechea, M.C.U. Araujo, B.S.F. Band, Successive projections algorithm improving the multivariate simultaneous direct spectrophotometric determination of five phenolic compounds in sea water, Microchem. J. 85 (2007) 194–200.

[18] M.F. Pistonesi, M.S. Di Nezio, M.E. Centurión, A.G. Lista, W.D. Fragoso, M.J.C. Pontes, M.C.U. Araújo, B.S.F. Band, Simultaneous determination of hydroquinone, resorcinol, phenol, m-cresol and p-cresol in untreated air samples using spectrofluorimetry and a custom multiple linear regression-successive projection, Talanta 83 (2010) 320–323.
[19] F. Allegrini, P.D. Wentzell, A.C. Olivieri, Generalized error-dependent prediction uncertainty in multivariate calibration, Anal. Chim. Acta 903 (2016) 51–60.
[20] C.M. Andersen, R. Bro, Quantification and handling of sampling errors in instrumental measurements: a case study, Chemom. Intell. Lab. Syst. 72 (2004) 43–50.
[21] MATLAB, Version 7.0, The Mathworks Inc., Natick, Massachusetts, 2010.
[22] P.D. Wentzell, M.T. Lohnes, Maximum likelihood principal component analysis with correlated measurement errors: theoretical and practical considerations, Chemom. Intell. Lab. Syst. 45 (1999) 65–85.
[23] P.D. Wentzell, Measurement errors in multivariate chemical data, J. Braz. Chem. Soc. 25 (2014) 183–196.
[24] M.N. Leger, L. Vega-Montoto, P.D. Wentzell, Methods for systematic investigation of measurement error covariance matrices, Chemom. Intell. Lab. Syst. 77 (2005) 181–205.